

NGU Report 98.077

Testing of hyperspectral scanner data for  
prospecting of ferro-eclogite in the Førdefjord  
area, Western Norway

Report no.: 98.077		ISSN 0800-3416	Grading: ÅPEN
Title: Testing of hyperspectral scanner data for prospecting of ferro-eclogite in the Førdefjord area, Western Norway			
Authors: Follestad, Bjørn and Korneliussen, Are		Client: The Sogn & Fjordane county v/Dep of regional policy and the Geological Survey of Norway	
County: Sogn and Fjordane		Commune: Naustdal	
Map-sheet name (M=1:250.000) Florø		Map-sheet no. and -name (M=1:50.000) 1118 II Eikefjord, 1117 I Dale	
Deposit name and grid-reference: Engjboe		Number of pages: 14	Price (NOK):
Fieldwork carried out: 1996		Date of report: 1998	Map enclosures: 0
Project no.:		Person responsible:	
2722.00		Nigel L. M.	
Summary: Remote sensing technology applied to resource monitoring has been carried out in the Engjebø mountain. These tests combines laboratory measurement of the reflectivity, field measurement and spectral data collected with an airborne hyperspectral scanner. Even though the field measurement on the ground indicted that a spectral separation should be possible, the spectral analyses collected by an aircraft with 10m x 10m resolution, do not give any clear detection of the rock-types. This is mostly thought to be caused by the vegetation in the area.			
Keywords: fjernalyse	prospektering	mineral	

## CONTENTS

Background for the use of remote sensing scanning techniques in an airborne scanning system	4
Remote sensing techniques in the Eggebø mountain, Førdefjord areas	5
1. Laboratory measurement of the reflectivity curves using the spectrometer at the Defence Research Laboratory	5
2. Measurement in the Englebø mountains, Førdefjord areas	8
3. Spectral data analysis of data collected with the airborne hyperspectral scanner	11
Conclusions	14

# Testing of hyperspectral scanner data for prospecting of ferro-eclogite in the Førdefjord area, western Norway.

In 1996 a covenant agreement for testing the potential of the hyperspectral scanner technique in an area in Sogn og Fjordane was established between the Sogn og Fjordane county (Department of regional policy) and the Geological Survey of Norway (NGU). The studies were related to on-going geological investigations in the Engjeboe mountain area in the Førdefjord district (Kornéliussen & Foslie, 1985) of western Norway (Fig. 1).

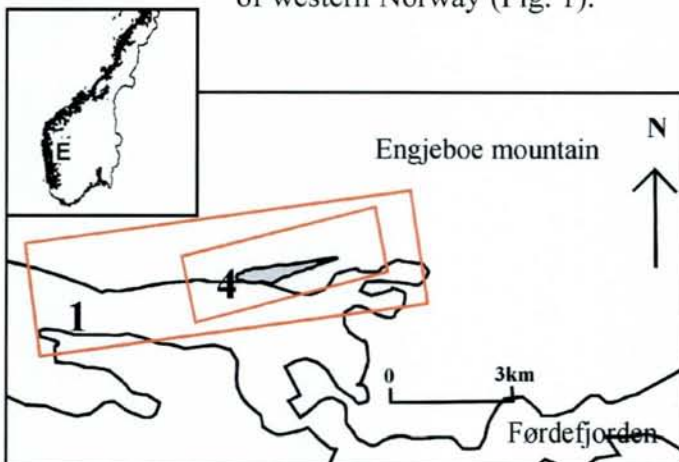


Fig. 1. Location of the hyperspectral scanner stripes, the Førdefjord district of western Norway. For more details concerning channels, see Table 2.

The Engjeboe eclogite deposit is situated at the northern side of Førdefjord near the small community Vevring in Naustdal kommune, Sogn og Fjordane county. Geologically the Førdefjord area belongs to the «Western Gneiss Region», between the Devonian Kvamshesten basin to the south and the Devonian Håsteinen basin to the North. The Førdefjord region consists of a variety of amphibolitic, eclogitic and gabbroic rocks, together with tonalitic, dioritic and granitic gneisses.

The Engjeboe eclogite is a 2.5 km long, complexly deformed, lens-formed body surrounded by alternating mafic-felsic country-rocks. The protolith to the eclogite is believed to be a Fe and Ti-rich Proterozoic gabbroic intrusion. The transformation into eclogite is related to Caledonian high-pressure metamorphism at approx. 400 Ma. In this process ilmenite in the gabbro protolith was replaced by rutile. The eclogite is subdivided into a leuco-eclogite and a ferro-eclogite variety. The ferro-eclogite, which is distinctly enriched in iron (>14% Fe<sub>2</sub>O<sub>3</sub>) and titanium (>3% TiO<sub>2</sub>, primarily as rutile), has been the target for rutile exploration at Engjeboe mountain.

The purpose of the present investigation is to investigate if remote sensing data can be used in future investigations for rutile-rich eclogite similar to the ferro-eclogite type of Engjeboe.

## Background for the use of remote sensing scanning techniques in an airborne scanning systems

Remote sensing technology applied to Earth resource monitoring and management have, on a global scale, gone on since the early in the 1970's when the first Earth Resource Satellite (ERS) was launched. This satellite, later renamed the "Landsat earth resources satellite", was the first of a series of five satellites designed to provide a near-global coverage of the Earth's surface on a regular and predictable basis. Later satellite systems, such as e.g. the SPOT, utilised the same bands.

The Landsat satellite has a sun-synchronous, near-polar orbit. Its altitude is 920 km, the orbital period 103 minutes and there are 14 orbits per day. In Landsat 1, 2 and 3, a multispectral scanner (MSS) and return beam vidicon (RBV) were the principal sensors. For Landsat 4 and 5 the Thematic Mapper (TM) sensor substituted the RBV and improved spectral, spatial and radiometric characteristics. Seven wavelength bands are used; 3 in the visible, three in the infrared (IR) and one band in the thermal part of the spectrum (Landsat 3).

For the construction of the MSS and the TM mechanical scanning instrument and to improve our understanding of the scanner data, it was necessary to devise and operate a similar scanner in the visible and infrared regions of the spectrum at aircraft altitudes. The best known aircraft scanner is the Daedalus AADS 1240/1260 multispectral line scanner. Such scanners permit data acquisition in a variety of waveband configurations. Image scanning is achieved by means of a rotating mirror from which reflected light is passed to the sensor via a series of mirrors and a diachronic lens. For the Daedalus scanner, available channels are in the ultraviolet, visible and reflective IR parts of the spectrum. Later the airborne multispectral line scanners, airborne thematic mapper (ATM) and thermal infrared multispectral

scanner (TIMS) and the MIDA MEIS-II linear array aircraft scanners have followed.

These developments in scanner technology, and in the subsequent processing of collected spectral information through data handling, have provided us the airborne systems and image-software packages used in this study.

As a basis for evaluating the remote sensing hyperspectral airborne scanner data, testing of the reflectiveness of minerals in rock samples has been carried out in the laboratory and in the field. These tests are described later.

### Remote sensing techniques in the Engjeboe mountain, Førefjord areas

The potential of hyperspectral scanner data for the identification of mineralised zones on the surface of the Earth has long been recognised in many parts of the world. In Norway, only a few studies have been carried out in geology, mostly dealing with the mapping of lineaments, surficial deposits and the natural and anthropogenic pollution of soil and vegetation, e.g., (Bølviken et al. (1977), Ridnstad & Follestad (1982), Rød (1992) and Roberts & Karputz (1995).

In 1996, a flight over a Norwegian test area in the Førefjord district was carried out on 18 July, using the Geophysical & Environmental Research Corporation's 63-channel scanner in a 31-channel digital mode (GER 63). The site is located in the area of Engjeboe mountain to the north of Førefjord (Fig. 1) and cover the elongate, eclogitised gabbroic intrusions containing enrichments in titanium and iron (Korneliussen & Foslie 1985, Lutro & Ragnhildstveit 1996).

Sample number	locality	Rock type	TiO <sub>2</sub>	Fe <sub>2</sub> O <sub>3</sub>	Comments to the rock samples
R1a1.96	Engjeboe	leuco-eclogite	0,5	10	light coloured rock, no moss on surface
R1a2.96	Engjeboe	leuco-eclogite	0,5	10	light coloured rock, no moss on surface
R1b1.96	Engjeboe	leuco-eclogite	0,6	11,8	light coloured rock, no moss on surface
R1b2.96	Engjeboe	leuco-eclogite	0,6	11,8	light coloured rock, no moss on surface
R3a1.96	Engjeboe	ferro-eclogite	3,2	16,9	dark coloured rock, no moss on surface
R3a2.96	Engjeboe	ferro-eclogite	3,2	16,9	dark coloured rock, no moss on surface
R3b1.96	Engjeboe	ferro-eclogite	3,4	18	dark coloured rock, no moss on surface
R3b2.96	Engjeboe	ferro-eclogite	3,4	18	dark coloured rock, no moss on surface
R3c1.96	Engjeboe	ferro-eclogite	3	17	dark coloured rock, no moss on surface
R3c2.96	Engjeboe	ferro-eclogite	3	17	dark coloured rock, some moss on surface
R5a1.95	Engjeboe	gneiss			light coloured rock, no moss on surface
R5a2.95	Engjeboe	gneiss			light coloured rock, no moss on surface
R6b1.96	Engjeboe	gneiss			light coloured rock, some moss on surface
R6b2.96	Engjeboe	gneiss			light coloured rock, no moss on surface
R7a1.96	Engjeboe	gneiss			
R7a2.96	Engjeboe	gneiss			

The tests consisted of three parts :

- (1) Laboratory measurement of the reflectivity curves using the spectrometer at the Defence Research Laboratory (Forsvarets forsknings institutt (FFI));
- (2) Field measurement using a portable spectral radiometer (GER 3700);
- (3) Spectral data analysis of data collected with the airborne hyperspectral scanner.

### (1) Laboratory measurement of the reflectivity curves using the spectrometer at the Defence Research Laboratory (FFI)

Spectral measurement of rock samples (Table 1) was carried out at the Defence Research Laboratory (FFI) using a Perkin-Elmer UV scanner. Each sample was treated separately and scanned in the waveband range of 480 microns to 3129 microns. The scanned data were standardised against Ba<sub>2</sub>SO<sub>4</sub>.2H<sub>2</sub>O reference value and stored in ASCII format. The results are shown as a mean value (gjsn) of reflectivity (%) to the spectral band from 500nm = 0.5

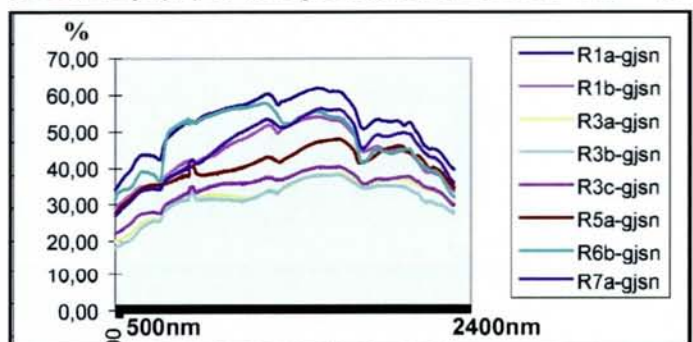


Fig. 2 Reflection of energy in % as a mean of measurement of two samples of each main rock samples of pectively leuco-eclogite (R1a, R1b), gneiss (R5a, R6b, R7a) and ferro-eclogite (R3a, R3b, R3c) compared to a standard of BaSO<sub>4</sub>. x-axis: microns from 0.4 to 25 microns.

Table 1. Rock samples collected and analysed in 1996 for content of TiO<sub>2</sub> and Fe<sub>2</sub>O<sub>3</sub> given as %.

microns (1microns = 1/1.000.000m) to 2400nm. As seen in the 2-D plot (Fig. 2) the percentage of reflections are up to 15 % higher for rock samples of leuco-eclogites (R1a-gjsn, R1b-gjsn) and gneiss (R5agjsn, R6bgjns, R7a-gjns) than in the rock samples of ferro-eclogite (R3a-gjn, R3b-gjns, R3c-gjsn).

To examine these reflection values more closely, the samples of leuco-eclogites (Fig.3 and Fig. 4), gneiss (Fig. 5 and Fig. 6) and ferro-eclogite (Fig 7 and Fig. 8) are shown in more detail. The sample numbers and the contents of TiO<sub>2</sub> and Fe<sub>2</sub>O<sub>3</sub> are related to in Table 1.

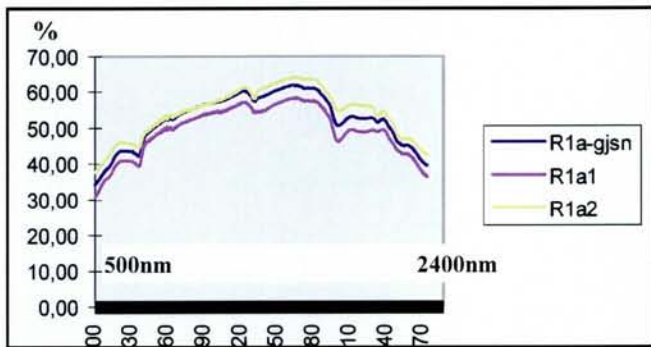


Fig 3. Reflected energy (%) of two sub-samples of a samples of leuco-eclogite (R1a1 and R1a2) compared to the mean of the measurement (R1a-gjsn).

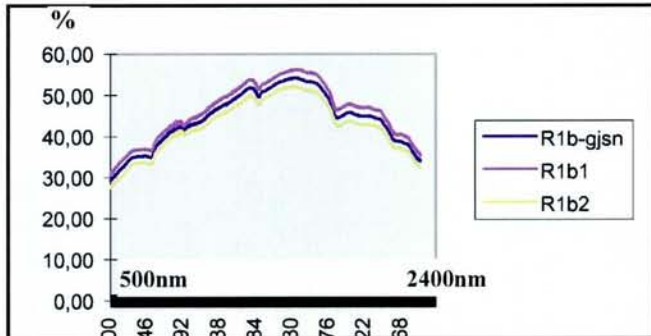


Fig 4. Reflected energy (%) of to sub-samples of leuco-eclogite (R1b1 and R1b2) compared to the mean of the measurement ( R1b-gjsn).

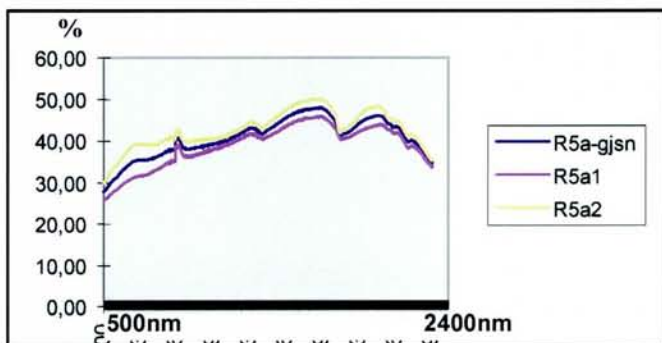


Fig. 5. Reflected energy (%) of two subsamples of a gneiss compared to the mean of the measurement (R5a-gjsn, R5a1 and R5a2).

### Leuco-eclogites (Figs. 3 and Fig. 4).

In the two samples of leuco-eclogites the TiO<sub>2</sub> and Fe<sub>2</sub>O<sub>3</sub> values are, respectively, 0.5% and 10% and 0.6% and 11.8%. The curves of reflectivity show almost the same patterns and peaks.

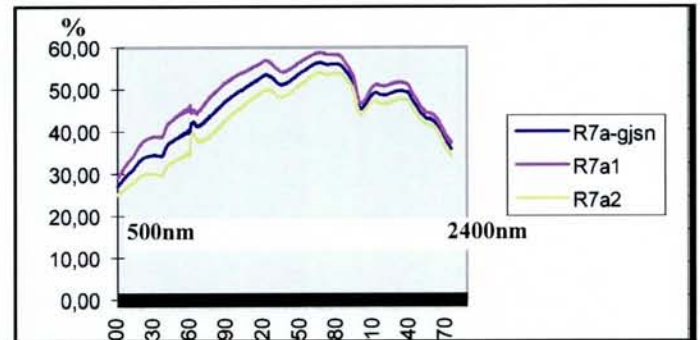


Fig. 6. Reflected energy (%) of two subsamples of a gneiss (R7a1 and R7a2) compared to the mean of the measurement (R7a-gjsn ).

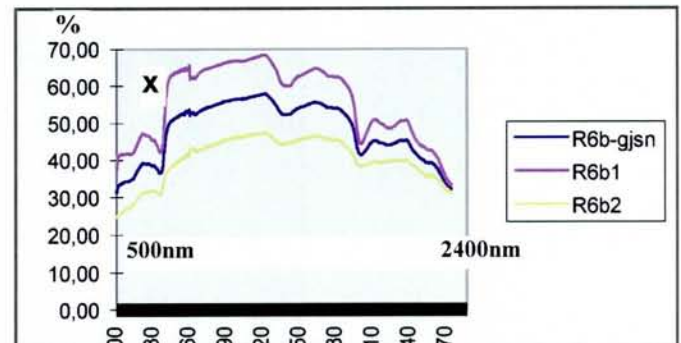


Fig. 7. Reflected energy (%) of two subsamples of a gneiss (R6a1 and R6a2) compared to the mean of the measurement (R6a-gjsn). These samples have some moss.

### Gneisses (Fig. 5, Fig. 6 and Fig. 7)

The pattern of reflectivity for some typical samples of gneisses are shown in Fig. 5 and Fig. 6. The curves R5a1 and R5a2 are subsamples of the same sample, are nearly identical. They can, however, hardly be separated from those of leuco-eclogites (se Fig. 3, R1a.96 and Fig. 4, R1b.96).

The gneiss samples R7, with subsamples R7a1 and R7a2, show the same value for reflectivities in the visible part of the spectrum as sample R5a. In the middle part of the infrared spectrum (900nm - 1800nm) the reflected value is somewhat higher than for the other gneisses.

The two samples of gneisses, R6b1 and R6b2 with and without some moss, are shown in Fig. 8. These curves clearly demonstrate that the reflectivity of sample R6b1 (and the mean R6b-gjsn) will be affected by the present of moss. The marked gradient of the reflection curves in the near infrared region (900nm)

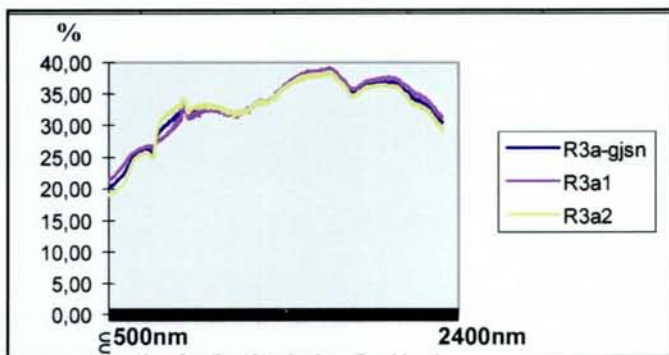


Fig. 8. Reflected energy (%) of two subsamples of a samples of a ferro-eclogite compared to the mean of the measurement (R3a-gjsn, R3a1 and R3a2).

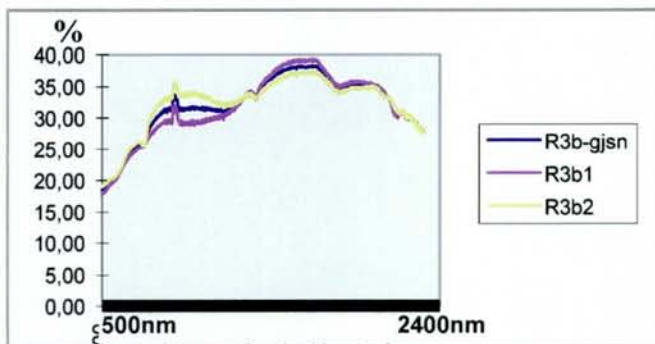


Fig. 9. Reflected energy (%) of two subsamples of a samples of a ferro-eclogite compared to the mean of the measurement (R3b-gjsn, R3b1 and R3b2).

are characteristic for chlorophyll, marked with "x". As the R6b2-sample has a lesser rise in the 900nm band, the measured part of this sample will have to be without moss (see table 1).

From this it can be concluded that moss on the surface will change the % of reflectivnes dramatically and give the reflectivity curve for chlorophyll (vegetation).

**Ferro-eclogite.** Four subsamples from two sites of ferro-eclogite R3a1/R3a2 and R3b1 and R 3b2 have been tested and the results are shown in Fig. 8 and Fig. 9. These samples having respectively a TiO<sub>2</sub>/Fe<sub>2</sub>O<sub>3</sub> content of 3,2%/16,9% and 3,4%/18,9%, show a rather similar spectrum of reflectivity.

The reflectivity curves for the ferro-eclogites are characterised by a rather low value of reflectivity in the visible part of the spectrum, ca. 20%. Compared to the spectrums of leuco-eclogites and gneisses this is a 10% reduction. The reduction of reflected energy are seen both in the visible and the infrared parts of the spectrum.

**Conclusion.** The laboratory tests appear to indicate that the rock surface of ferro-eclogite will generally have a lower reflectivity compared with the surface of leuco-eclogite and gneiss. However, the presence of moss on the surface will change these characteristics.

## References

- Bølviken, B., Honey, F, Levine, R. Lyon, R. Prelat, A. 1977: *Detection of natural heavy-metal-poisoned areas by Landsat-1 digital data.* Jour. Geoch. Exploration, 8 , 457-471.
- Drury, S.A. 1987: *Image Interpretation in Geology.* Allen & Unwin (Publishers) LTD. ISBN 0-04-550037-1.
- Karputz, R., Roberts, D. Moralev, D.V & Terekhov, E. 1995: *Regional lineaments of eastern Finnmark, Norway, and the Western Kola Peninsula, Russia.* Nor.geol.unders. Special Publ. 7, 121-135.
- Korneliusson, A.. & Foslie, G. 1985: *Rutile-bearing eclogites in the Sunnfjord region of Western Norway.* Nor. geol. unders. 402, 65-71.
- Lutro, O. & Ragnhildstveit, J. 1996: *Geologic map of the Førdefjord area, bedrock map, scale 1:50.000.* Unpublished NGU.
- Richards, J.A.1986: *Remote Sensing Digital Image Analysis.* ISBN 3-540-16007-8, Springer-Verlag, Berlin, Heidelberg, New York.
- Rindstad, R. & Follestad, B.A. 1982: *Digital methods for lineament analysis.* First Thematic Conference: Remote Sensing of Arid and Semi-Arid Lands, Cairo, EGYPT
- Roberts, D. & Karputz, M.R. 1995: *Structural features of the Rubachi and Sredni Peninsulas, Northwest Russia, as interpreted from Landsat - TMimagery.* Nor.geol.unders. Special Publ. 7, 145-150.
- Rød, J.K 1992: *Perspektivisk visualisering av et SPOT-bilde samregistrert med geologisk tema.* Nor. geol.unders. Rap. 92.256

## (2) Measurements in the Engjaboe mountains, Førdefjord area

The GER Mark V spectrometer is a portable instrument for measuring reflected electromagnetic energy. It operates in the visible and infrared parts of the spectrum, from 300 to 2500 nm (or 0.3 to 25 microns). The spectral resolution is 10 nm with a sampling interval of 2 nm. A BaSO<sub>4</sub> plate is used as a standard for the instrument, and the BaSO<sub>4</sub> values are given together with the spectral readings at the measured site. This BaSO<sub>4</sub>-standard allows for a normalisation of site readings, as we shall see later. Hopefully these spectral tests will give a possibility for separating the different rock types in the area (Hummer-Miller & Watson 1997, Kale & Rown 1980).

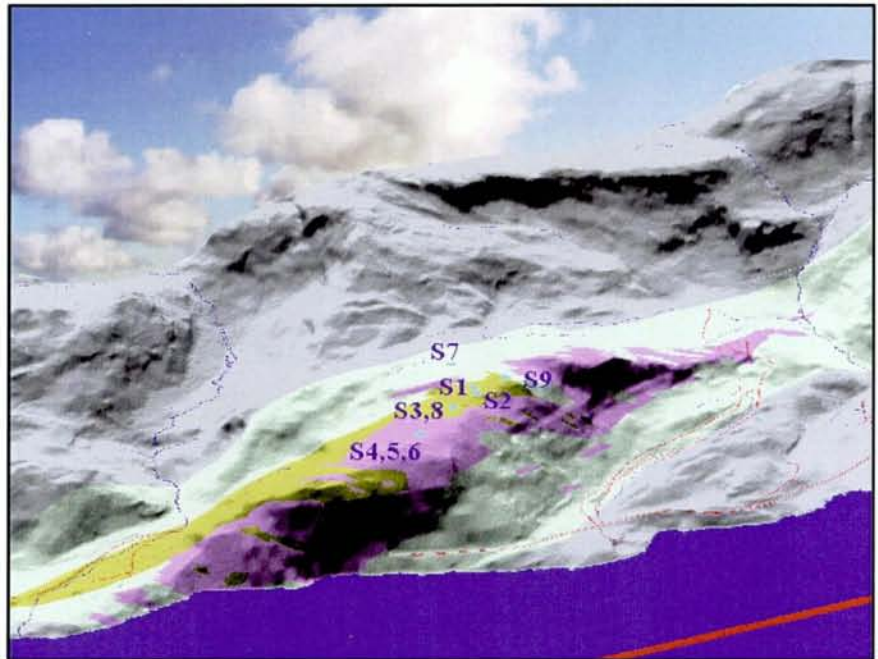


Fig. 10. The Engjaboe mountain shown in 3-D, with the major rock units and the location sites for sampling of reflected informations (S1 - 11, for more information see Table 2). The central part of the image shows ferro-eclogite in violet, leuco-eclogite in yellow, amphibolite in light green and gneiss in grey. The red line indicates a distance of ca. 1 km. The model is made by use of the Intergraph Vaxel Analyst with grid resolution 5 m x 5 m, Eyolf Erichen, NGU 1998.

Table 2. Samples localities for field investigations 11. Aug. 1996

Locality	Rock	% TiO <sub>2</sub>	% Fe <sub>2</sub> O <sub>3</sub>	UTM-East	UTM-North	Spectral measurement, Engjaboe mountain 11. aug. 1996				
						Measure	Level [m]	#0 dB Detector	Time	File name
S1	Leuco-eclogite	1,23	11,74	310589	6823337	0	0,6	OFF	933	S1M0.SIG
S1	Leuco-eclogite	1,23	11,74	310589	6823337	1	0,6	OFF	935	S1M1.SIG
S1	Leuco-eclogite	1,23	11,74	310589	6823337	2	0,6	ON	939	S1M2.SIG
S1	Leuco-eclogite	1,23	11,74	310589	6823337	4	0,6	OFF	949	S1M4.SIG
S1	Leuco-eclogite	1,23	11,74	310589	6823337	5	0,6	ON	956	S1M5.SIG
S2	Leuco-eclogite	1,17	12,14	310587	6823307	0	0,6	OFF	1015	S2M0.SIG
S2	Leuco-eclogite	1,17	12,14	310587	6823307	1	0,6	OFF	1020	S2M1.SIG
S3	Leuco-eclogite	1,16	10,66	310490	6823273	0	0,6	OFF	1039	S3M0.SIG
S3	Leuco-eclogite	1,16	10,66	310490	6823273	1	0,6	OFF	1044	S3M1.SIG
S4	Ferro-eclogite	4,27	14,28	310350	6823191	0	0,6	OFF	1101	S4M0.SIG
S4	Ferro-eclogite	4,27	14,28	310350	6823191	1	0,8	OFF	1105	S4M1.SIG
S5	Ferro-eclogite	4,03	13,95	310350	6823184	0	0,8	OFF	1126	S5M0.SIG
S5	Ferro-eclogite	4,03	13,95	310350	6823184	1	0,8	OFF	1131	S5M1.SIG
S6	Ferro-eclogite	4,36	12,93	310348	6823187	0	0,7	OFF	1114	S6M0.SIG
S7	Amfibolite			310575	6823470	0	0,6	OFF	1155	S7M0.SIG
S7	Amfibolite			310575	6823470	1	0,6	OFF	1157	S7M1.SIG
S7	Amfibolite			310575	6823470	2	0,6	OFF	1200	S7M2.SIG
S8	Amfibolite			310578	6823472	0	0,8	OFF	1206	S8M0.SIG
S8	Amfibolite			310578	6823472	1	0,8	OFF	1208	S8M1.SIG
S8	Amfibolite			310578	6823472	2	0,8	OFF	1212	S8M2.SIG
S8	Amfibolite			310578	6823472	3	0,8	OFF	1215	S8M3.SIG
S9	gneiss			310695	6823340	0	0,6	OFF	839	S9M0.SIG
S9	gneiss			310695	6823340	1	0,6	OFF	845	S9M1.SIG
S9	gneiss			310695	6823340	2	0,6	OFF	856	S9M2.SIG
S9	gneiss			310695	6823340	3	0,6	OFF	900	S9M3.SIG
S9	gneiss			310695	6823340	5	0,6	OFF	902	S9M5.SIG
S9	gneiss			310695	6823340	6	0,6	OFF	905	S9M6.SIG
S9	gneiss			310695	6823340	7	0,6	ON	908	S9M7.SIG
S9	gneiss			310695	6823340	8	0,6	ON	911	S9M8.SIG



The working spectral range of the instrument GER Mark V is in the same wavelength as the GER 63-channel imaging spectrometer (operated in 31-channel operating mode) which was flown over the area in July 1996.

Due to various problems and some delays in customs clearance, the field work using the GER Mark V spectrometer was not carried out until 11 August 1996. At this time of the year, however, the variations in incoming electromagnetic energy are not considered to have any major influence on spectral measurements. In our case the time of the day when the measurements were taken (from 08.40 a.m. to 03.33 p.m.) together with the moisture content of the air constitute greater sources for deviation. No corrections have been made for potential changes in measurement due to day and month.

In the following account, some of the measurements carried out in the field at locality S1, S2, S3, S4, S5 and S6 will be discussed. For the remaining measurements, the readings give very much the same information, and are therefore left out of this description.

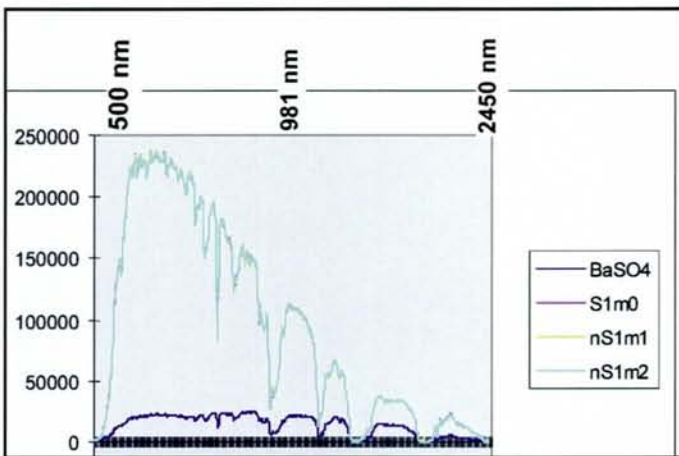


**Fig. 11.** Three parallel readings from sample site S1 of leuco-eclogite. Samples S1m1 and S1m2 are normalised to sample S1m0 by multiplying the observed values with ratio of the BaSO4 for S1m0/S1m1 and S1m0/S1m2, respectively. The BaSO4 curve for S1m0 is given as a reference.

**Sample locality S1 (leuco-eclogite)** Three parallel readings were taken from 09.33 a.m. to 09.56 a.m. at site S1. The surface of the rock is described as a massive leuco-eclogite with TiO<sub>2</sub> and Fe<sub>2</sub>O<sub>3</sub> contents of 1.23 % and 11.74%, respectively. The site is well exposed, with only very little moss vegetation. The separate readings of S1m0, S1m1 and S1m2 (the readings of S1m1 and S1m2 are normalised to S1m0 values) and the results are shown in Fig 11.

On the basis of these measurements, normalised with respect to the readings of BaSO<sub>4</sub> sample S1m0, the curves indicate that a surface of massive leuco-eclogite with little moss, has a rather constant reflectivity

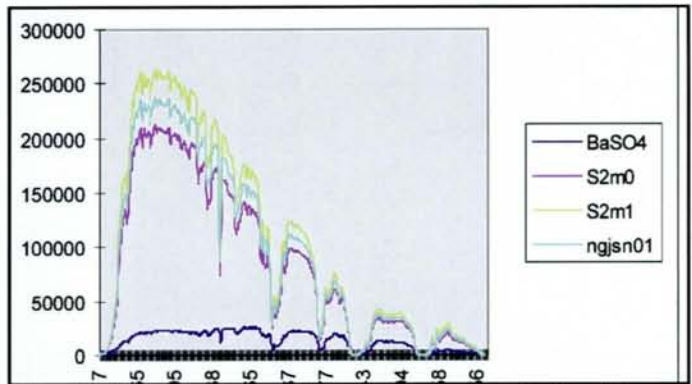


**Fig. 12.** Two parallel readings from sample site S2 of leuco-eclogite. A normalization is carried on sample S2m1, to make it comparable to sample S2m0 (as described above in Fig. 11). The mean is shown as a mean of S2m0 and a normalised S2m1. The BaSO<sub>4</sub> curves for S2m0 are given as a reference. For scale information on the x-axis, see Fig. 11.

in the visible and infrared parts of the spectrum.

**Sample locality S2 (leuco-eclogite).** Two parallel readings were taken at site 2S from 10.15 a.m. to 10.20 a.m. The rock surface there is a massive leuco-eclogite with TiO<sub>2</sub> and Fe<sub>2</sub>O<sub>3</sub> contents of 1.17% and 11.74%. The site is well exposed, with only negligible moss vegetation. The readings of S2m0 and S2m1 (the readings of S2m1 are normalised to S2m0) are shown in Fig. 12. From the curves it can be seen that S2m1 will have more light moss vegetation than S2m0, as it is reflecting more in the near infrared part of the spectrum (700 nm to 1100 nm). No distinctions were, however, made in the field descriptions with regard to the small changes in vegetation cover.

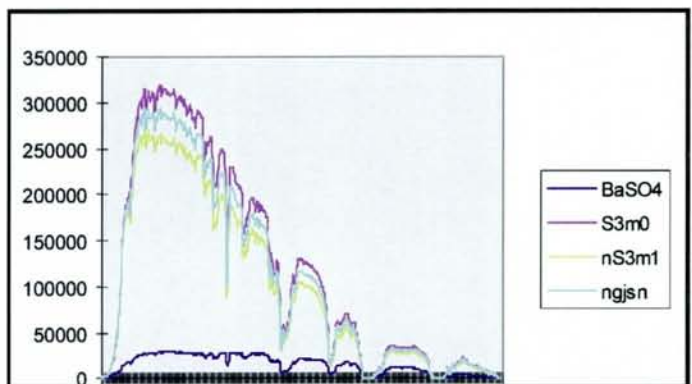


**Fig. 13.** Two parallel readings from sample site S3 of leuco-eclogite. A normalization is carried out on sample S3m1, to make it comparable to sample S3m0 (as described above in Fig. 11). The mean is shown as a mean of S3m0 and a normalised S3m1. The BaSO<sub>4</sub> curves for S3m0 is given as a reference. For scale information on the x-axis, see Fig. 11.

**Sample locality S3 (leuco-eclogite).** Two parallel readings were taken from 10.39 a.m. to 10.44 a.m. The rock-type at the site is described as a foliated leuco-eclogite. No comments were made on the moss vegetation. As can be seen (Fig. 13), the values are

somewhat higher than those at site S2.

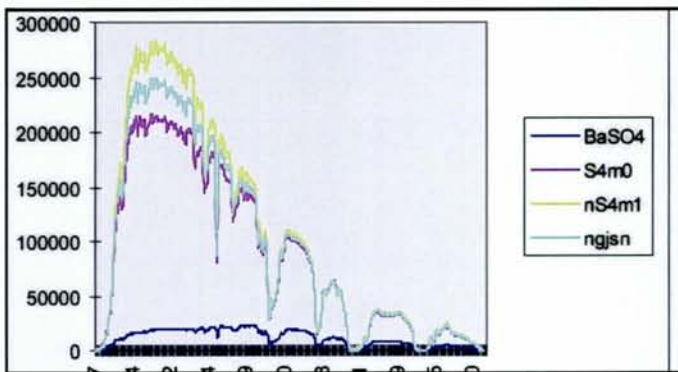


Fig. 14.. Two parallel readings from sample site S4 of ferro-eclogite. A normalization is carried out on sample S4m1, to make it comparable to sample S4m0 (as described above in Fig. 11). The mean is shown as a mean of S4m0 and a normalised S4m1. The BaSO4 curves for S4m0 is shown as a reference. For scale information on the x-axis, see Fig. 11.

**Sample locality S4 (ferro-eclogite).** Two parallel readings were taken from 10.39 a.m. to 10.44 a.m. of a massive ferro-eclogite with TiO<sub>2</sub> and Fe<sub>2</sub>O<sub>3</sub> contents of 4.27% and 14.28%, respectively. There is some moss on the surface. The separate readings of S4m0, S4m1 (the readings of S4m1 are normalised to S1m0 values) and the mean (ngjsn) are shown in Fig. 14. The yellow curve (nS4m1) peaks in the area of 550 nm and is also higher in the near infrared than the red curve (S4n0). This indicates a site richer in moss. In the middle- and extreme infrared part of the spectrum, the curves with this resolution used in Fig. 14, give no evidence for separation. This is discussed later, see Fig. 16 and Fig. 17.

**Sample locality S5 and S6 (ferro-eclogite).** Two parallel readings were carried out in sample locality

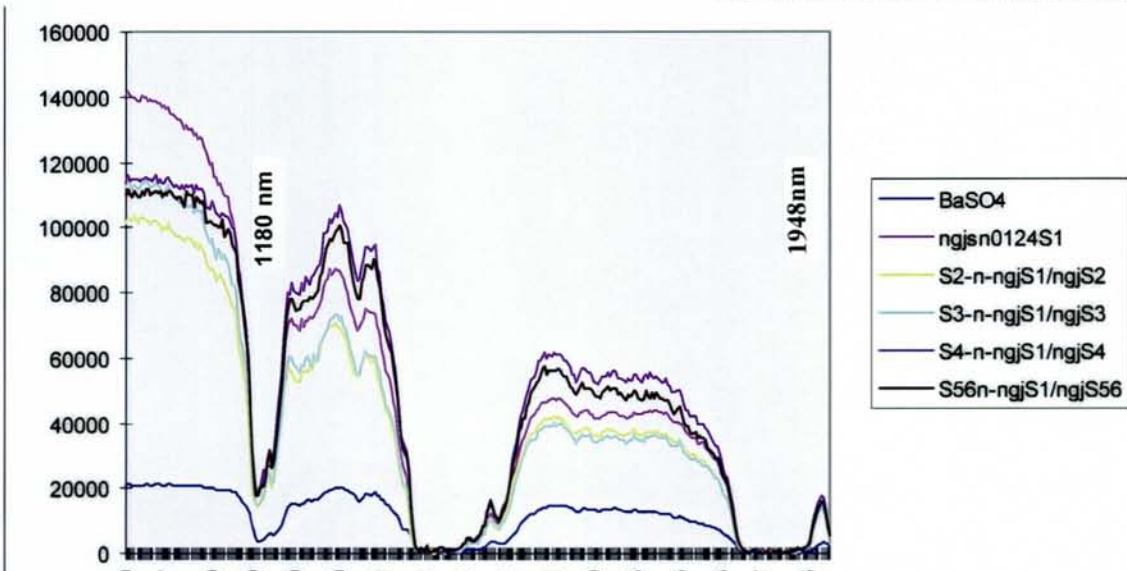


Fig. 16. The normalised value for the sample sites S1, S2, S4, S5 and S6 normalised to the value of S1. a The reflectivity of ferro-eclogite (brown curves) has higher reflectivity than the gneiss and probably also the leuco-eclogite (S1, S2,S3) in the wavelength region of 1180-1948nm.

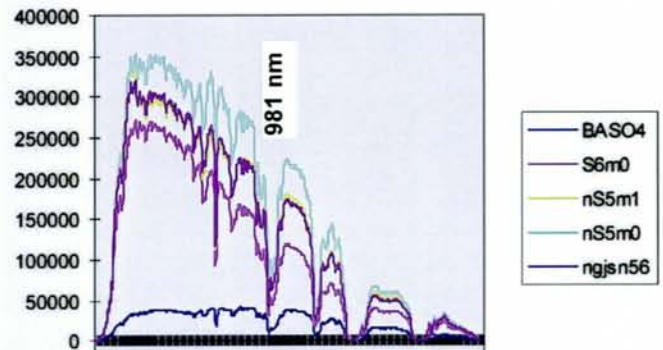


Fig. 15. Two parallel readings from sample site S5 and one reading from sample S6 of ferro-eclogite are shown. A normalization was carried out on sample S5m0 and S5m1, to make them comparable to sample S6m0 (as described above in Fig. 11). The mean ngjsn56-curve are the readings for S6m0 and the normalised values for S5m0 and S5m1. The BaSO4 curves for S6m0 is given as a reference. For scale information on the x-axis, see Fig. 11.

S5 and one reading in locality S6. The measurements (readings) were taken from 11.46 a.m. to 11.31 a.m. The sampling localities have some moss vegetation, which will effect the readings. The content of TiO<sub>2</sub> and Fe<sub>2</sub>O<sub>3</sub> are for S5 and S6 4,03% and 13,95% and 4,36%/12,93%, respectively (see Table 2). The results shown in Fig. 15, indicate that the separation of the rock types will be strongly affected by the cover of moss vegetation.

**The spectrum information bases on the GER Mark V.** In Fig. 16 and Fig. 17 a comparison of the normalised measurements is shown for the areas of 1180 nm - 1948 nm and 2000nm - 2497 nm. These enlarged diagrams of the field measurements indicate that the rock surface of ferro-eclogite appears to have the higher reflectivity in the areas of 1180 - 1948 nm. In the wavelength 2000 - 2497 nm the reflectivity seem to be general lower, see Fig. 17.

These characteristics can, however, not be used as the possible setting of the channels do not cover the 1180 nm - 1948 nm region of the spectrum, see Table 3.

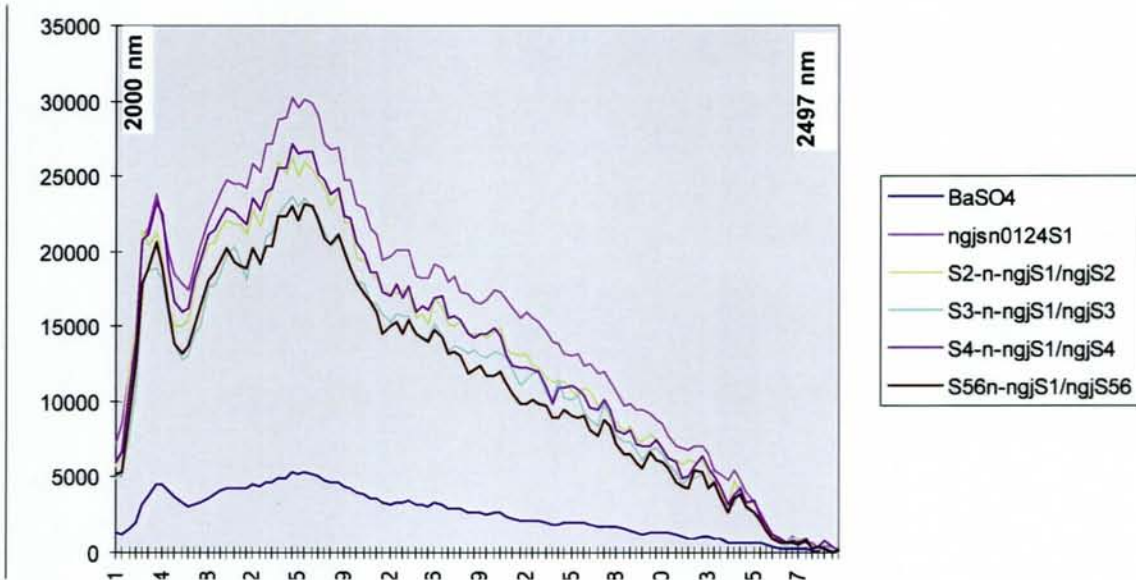


Fig. 17. The normalised value for the sample sites S1, S2, S, S5 and S6 compared to the value of sample site S1. The sites of ferro-eclogite (brown curves) has lower reflectivity and the gneiss and probably also the leuco-eclogite (S1, S2,S3) in the wavelength region of the spectrum.

### Conclusions

The reflection values (%) from the different parts of the spectrum seem to indicate that it is possible to discriminate between areas characterised by gneiss, leuco-eclogites and ferro-eclogites by using the spectral properties in the areas of 1180-1948nm.

### References

Hummer-Miller, S. Watson, K. 1997. *Evaluation of algorithms for geologic thermal inertia mapping*. Proc. 11th. Int. Symp. on Remote Sensing of Environment 1147-60.

Kale, A. B. & Rown, L.C. Evaluation of multispectral middle infrared aircraft images for lithologic mapping in the east Tonic Mountains, Utha. *Geology* 8, 234-239.

### (3) Spectral data analysis of data collected with the airborne hyperspectral scanner

The GER 63-channel imaging system is a airborne spectrometer. Measurements carried out in the ultraviolet, visible, infrared, and thermal parts of the spectra. The maximum number of channels for use in the scanner system is 63.

In the Norwegian tests, 31-channels have been in operating mode and one channel (32) is used for gyro. The channels used are shown in Table 3.

**Pre-processing of the data.** The data have been sub-

ject to minimal processing. Basic data processing consists of gyro, baseline correction and panoramic corrections. Gyro correction is carried out to remove the effects of the aircraft motion by translating each scanline horizontally in space by an amount proportional to the number of gyro counts. The gyroscope encodes the amount of aircraft roll in the last channel.

In the image, straight features within the image (such as roads) are straight, but the edges of the image may have irregular boundaries due to aircraft roll. Each scanline is translated an integral number of pixels to the right or left; there is no resampling. The spectral content of the data is unaffected by gyro correction.

Baseline correction utilises on-board reference panels to normalise the effects of detector reference voltages. When targets with extreme radiance differences are imaged, the GER scanner utilise a time-varying reference voltage to increase the effective dynamic range. The image of the baseline strip records the digital counts of a constant-reflectance panel. In baseline correction, the reference panel images are used to normalise the data so that the constant-reflectance panels have a

Channel	Band (nm)
1	410.0
2	432.0
3	483.6
4	521.3
5	565.8
6	617.7
7	665.8
8	716.6
9	768.5
10	823.7
11	883.9
12	941.9
13	989.7
14	1048.3
15	2039.3
16	2084.0
17	2112.5
18	2145.2
19	2170.0
20	2208.0
21	2237.7
22	2270.7
23	2296.2
24	2333.3
25	2358.0
26	2388.6
27	2411.7
28	2446.9
29	9468.4
30	10206.5
31	10983.1
32	Gyro

Table 3. Channels and band (Nm) for the GER 63 scanner in a 31-channel mode.

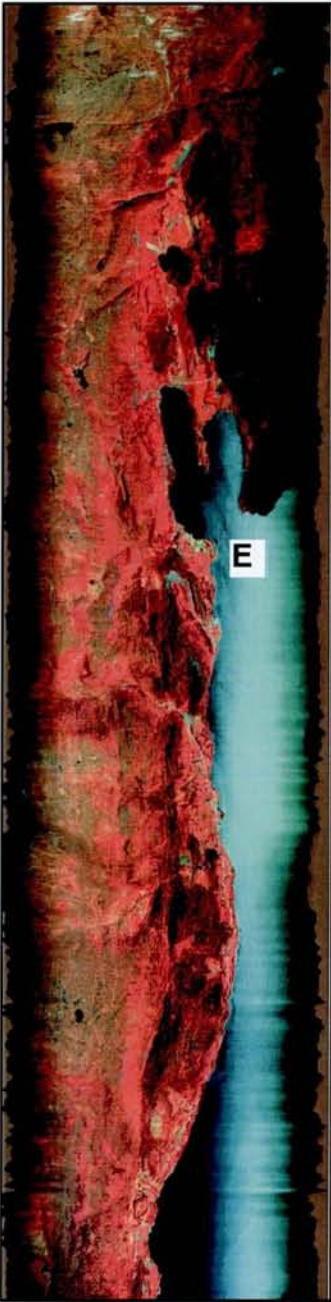


**Fig. 18. Test flight line 1. The Engjeboe test area shown as an RGB-colour image, Channel (ch) 13 red, ch 6 green 4 blue. Engjeboeneset is marked (E).**

constant digital count in the image. Each line and each channel are normalised individually. The 32 baseline pixels are removed from the data set.

Panoramic correction corrects the geometric distortions caused by the different viewing geometry in different parts of each scanline. Pixels are re-mapped into their correct position using nearest-neighbour resampling where possible, and linear interpolation where new pixels must be created. The spectral content for the nearest neighbour pixels is unaffected by panchromatic correction.

The data are delivered on 8 mm (Exabyte) tape and were written using the UNIX "tar" command on a Sun workstation. The basic flight strip is a single file with 16-bit unsigned integer

data in band-sequential (BSQ) format. Each file is accompanied by a headerfile (filemane.hdr) that gives the number of pixels per line, number of lines, etc. The header files are compatible with ENVI image processing software. The pre-processing has been designed to make the data ready for analysis and interpretation with delivery.

It should, however, be noticed that the chosen possible channels (Table 1) do not favour detection of ferro-eclogites in the 1000 nm - 1948 nm of the spectrum, as there is only one channel in this range (see table 3 channel 14).

**Spectral processing and analysis**

The ENVI software (the Environment for Visualizing Images, 2.7) is used for the image processing and classification of multispectral analysis of the aircraft

remote sensing data. The image processing system (ENVI) use a generalised raster data format stored as binary stream of bytes in band-sequential (BSQ) format. The basic function starts with an open image file where the different bands can be presented alone (as a grey scale image) or combined (as an RGB-colour image) as shown in Fig. 18.

This gives us the possibilities of combining channel (ch) 5 (blue), ch 8 (green) and ch 13 (red) and create a false colour image (RGB). This colour combinations shows us that the area is heavily vegetated as the reflected infrared ch 13 dominates the image. Some blue and green colours are chosen for channels (ch 5 and ch 8) with low reflectivity due to absorption in chlorophyll, the blue/green colour show areas with barren rock (the fjord would have

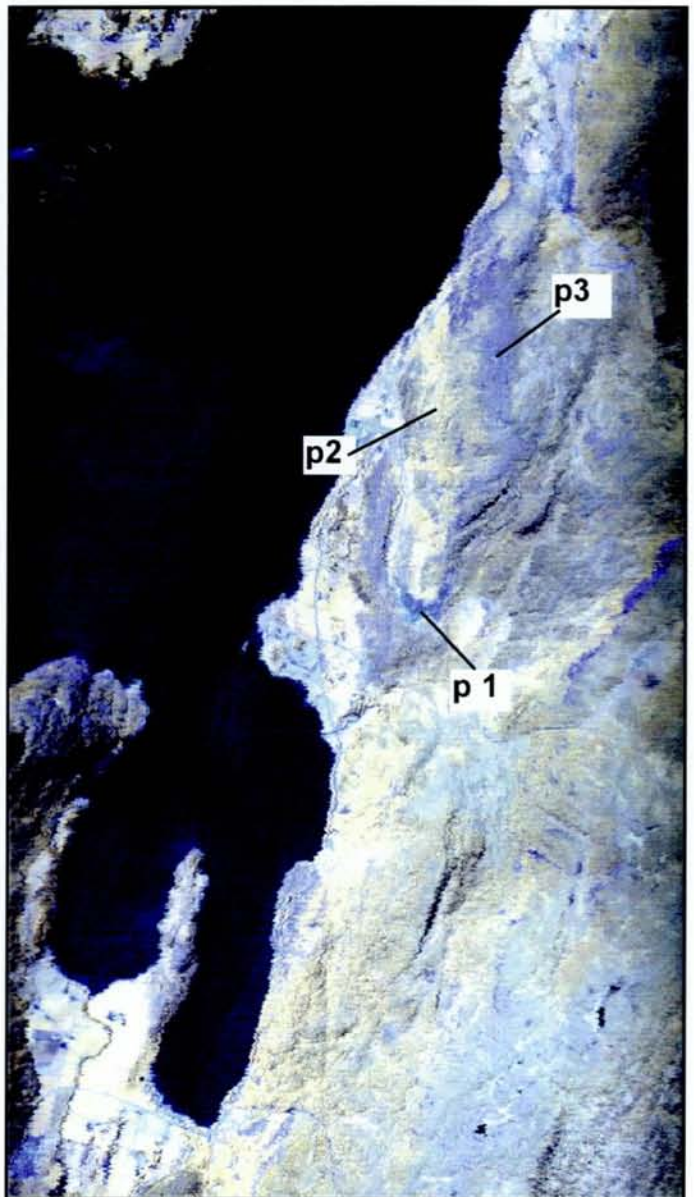


**Fig. 19. Barren rock surface (p 1), nearly barren rock surface (p3) and an area dominated by vegetation (p2) are shown in a spectral plott (Fig. 20).**

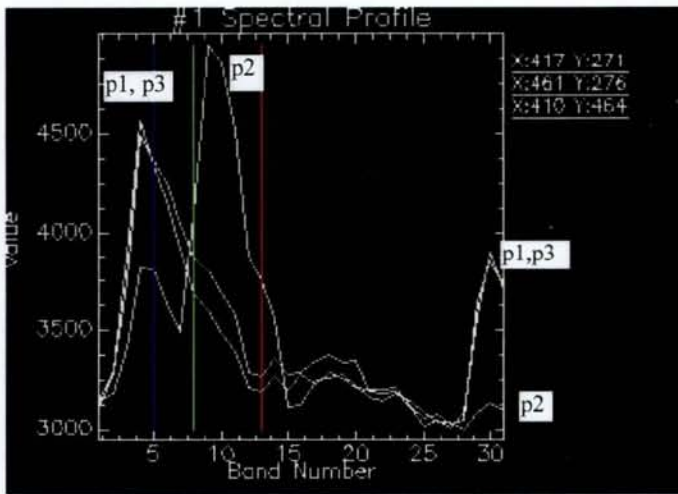


Fig. 20. RGB-composite of ch 5, ch 8 and ch 13, scanner flight 4 (Fig. 1) with location marks for spectral plots shown in Fig 8.

no chlorophyll in this connection. This indicates that it is only in the elevated parts of the area that we can expect a rock-surface, with little or no vegetation.

**Flight line 4**

A RGB-composite of ch 5, ch 8 and ch 13 is shown (Fig. 20), based on data from flight line 4 (Fig. 1).

The variance in the spectral reflectivity of all 31 channels, for test sites of nearly barren rock surface (p 1), barren rock surface (p 2) and an area dominated by vegetation (p 3) are shown in a spectral plot (Fig. 20).

Here it is clearly shown that the vegetated site (p2) has a maximum of reflection in areas of ch 10, equal to 823 nm. The barren rock surface (p1, p2) shows a maximum value in the areas of ch 4, equal to 521 nm.

In the areas from 1500 to 2400 nm, the curves of reflections are quite similar. In the thermal channels (ch 29, ch 30 and ch 31), however, there seems to be a higher value of thermal radiation for barren rock samples. This might be explained as a result of trapping of radiant energy (greenhouse effect) under a cover of leaves. Thermal radiation might, as we will see, be one channel of information which permits a classification.

**Classification of the region of interest (ROI), test flight 4 (Fig.1)**

The classification menu in ENVI software gives access to supervised and unsupervised classification. Utilities are also provided for: i.e., end-member collection, classifying previous rule images, calculating class statistics, etc. Supervised techniques use the endmember collection utility to import training class

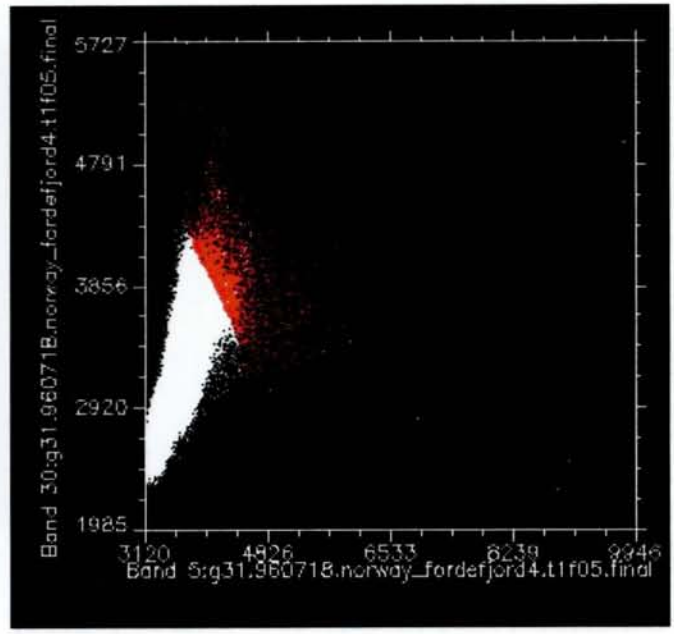


Fig. 21. Scatter plot of the minimum noise fraction (MNF) transformation used to determine the inherent dimensionality of ch 5 and ch 30.

spectra or ENVI's integrated region-of-interest (ROI) selection utilities to interactively define training classes. The selection routines allow extraction of training statistics from polygons, vectors, etc.

The minimum noise fraction (MNF) transformation can be used if a quick classification is wanted, as in our case. This transformation is used to determine the inherent dimension of image data, to segregate noise in the data, and reduce the computational requirements for subsequent processing as shown by Boardman and Kruse (1994).

In this work, the channel information for barren rock or nearly barren rock surfaces (marked with p1, p3, Fig. 20) and vegetation (p2, Fig. 20) are used for separation. These properties in ch 5 and in the thermal ch 30 for the respectively curves, give us a 2-axes diagram (Fig. 21).

In the algorithms on which this diagram is based, different transformations are carried out. The first transformation is based on an estimated noise covariance matrix, which decorrelates and rescales the noise in the data. This results in transformed data in which the noise has unit variance and no band-to-band correlation. The second transformation is a standard principal components transformation of the noise-whitened data. Thus the data space can be divided into one part assisted with large eigen-values and coherent eigenimages, and a complementary part with near-unity eigen-values and noise-dominated images. Classifying the data set by marking the area of interest through a "try and failure procedure" make the best fit possible. In Fig. 21 the selected data-points are shown (in red) and superimposed

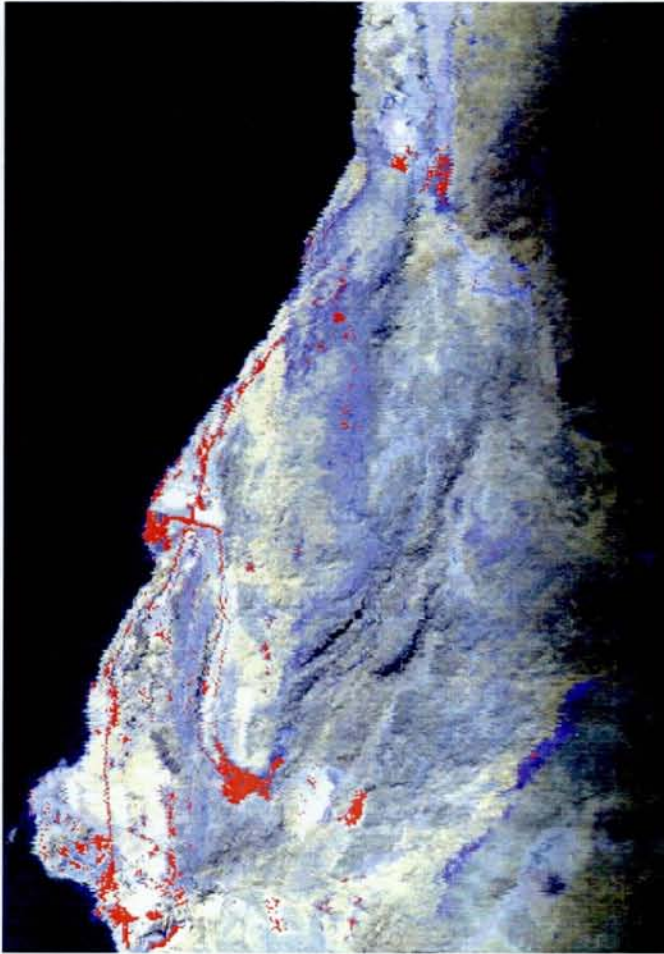


**Fig. 22.** The region of interests with the superimposed scatter plot, see Fig. 21.

onto the colour image in Fig. 22. Here it is clearly illustrated that this classification easily picks out the non-vegetated areas. These areas, such as roads and barren rock surfaces are readily seen. A comparison of the areas with gneiss and leuco-eclogite shows, however, that there is no separation of the different rock types.

### **Conclusions**

The reflection values (%) from the different parts of the spectrum seem to indicate that it is possible to discriminate between areas of vegetation and barren rock surface. However, the area is too heavily vegetated for a closer separation based on this scanner resolution 10m x 10m.

**Acknowledgements.** - We wish to thank Benny Moeller Soerensen (GER-INTRADAN A/S) and Prof. Brian Sturt for valuable cooperation.

### **References**

Boardman and Kruse (1993), F. A. & Lefkoff, A. 1993. *Knowledge-based geologic mapping with imaging spectrometers: Remote Sensing Reviews, Special Issue on NASA Innovative Research Program (IRP) results*, vol. 8, 3-28.